Statistical analysis of radar reflectivities observed and simulated by EMVORADO

Virginia Poli[1], Thomas Gastaldo[1,2], Pier Paolo Alberoni[1] and Tiziana Paccagnella[1][1]
Arpae-SIMC Emilia-Romagna, Bologna, Italy
[2] *Universitá degli Studi di Bologna, Bologna, Italy*

1 Introduction

In the COSMO Consortium (Consortium for Small-scale Modeling), the assimilation of radar data is now on-going into the Kilometer-scale ENsemble Data Assimilation (KENDA) LETKF system [1] by means of the Efficient Modular VOlume RADar forward Operator (EMVORADO, [2], [3], [4], [5], [6]). At Arpae-SIMC, the HydroMeteorological and Climate Service of the Emilia-Romagna (Italy), the attention is focused on the assimilation of radar reflectivity volumes.
The off-line version of EMVORADO, i.e. not included in the assimilation cycle, has been implemented to calculate the reflectivity volumes from KENDA analyses in order to estimate the observation error by means of a method based on statistical averages of observation-minus-background and observation-minus-analysis residual.As a side result, the comparison between the observed and simulated reflectivities allows us to understand how much the values derived by the operator deviate from reality. Hence, the use of the off-line operator makes it possible to verify how the reflectivity distributions vary both using different analyses, coming from various KENDA configurations, and by directly modifying the parameters of the operator himself.

2 Statistical distributions of reflectivities

To quantify the differences between reflectivities simulated with different EMVORADO configurations and also between observed and simulated ones, the off-line radar operator was applied, i.e. separately from the assimilation cycle, to all the analyses obtained from different assimilation cycles of KENDA. In particular, for this topic, hourly analyses come from KENDA with the assimilation of conventional observations (SYNOP, TEMP and AIREP) and KENDA with the assimilation of conventional observations and radar reflectivity volumes. The radar operator configurations that have been tested are summarized in table 1. Among all the possible combinations, the different type of scattering (Mie/Rayleigh) for reflectivity computation has been used. Subsequently, the attenuation along the beam was also taken into account for the Mie scattering. This option cannot be used for Rayleigh scattering. With regard to Rayleigh scattering, the effect of the use of different beam propagation methods has been verified. By default, the "4/3-earth" climatological model is used, the other two options enable the ray tracing and the beam bending computations based on the simulated air refractive index field [5]. Specifically the TORE method is based on Snell's law for spherically stratified media including effects of total reflection, while the SODE method is based on the second-order ordinary differential equation for the beam height as a function of range.

Table 1: EMVORADO configurations

Name	**Scattering options**	**Propagation options**
Mie	Mie scattering	Climatological "4/3-earth" model
Mie_atten	Mie scattering taking into account attenuation along the ray path	Climatological "4/3-earth" model
Rayleigh	Rayleigh scattering	Climatological "4/3-earth" model
Rayleigh_sode	Rayleigh scattering	Method SODE based on the second-order ordinary differential equation for the beam height as function of range
Rayleigh_tore	Rayleigh scattering	Method TORE based on Snell's law for spherically stratified media including effects of total reflection

doi:10.5676/dwd_pub/nwv/cosmo-nl_19_02

Once all the simulated volumes were produced, reflectivities above 0 dBZ were considered and boxplots were generated independently for the case studies indicated in table 2 (Figures 1 and 2). The choice to calculate the statistical distributions according to the events was due to the fact that the chosen periods have very different weather characteristics.

Table 2: Case studies

Event	Start of the event	End of the event	Type of event
September 2018	31/08/2018 01 UTC	09/09/2018 00 UTC	thunderstorms
October 2018	30/09/2018 16 UTC	14/10/2018 00 UTC	thunderstorms and organized convective structures
November 2018	26/10/2018 13 UTC	11/11/2018 00 UTC	stratiform structures with some convective episodes at the beginning of the period

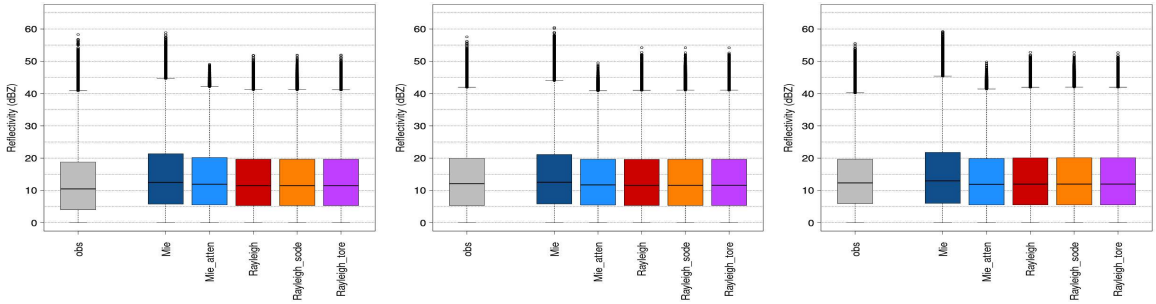

Figure 1: Boxplots calculated for September 2018 (a), October 2018 (b) and November 2018 (c) with input analyses from KENDA cycles with the assimilation of conventional observations.

Using as input analyses those derived from KENDA cycles with the assimilation of only conventional observations (Figure 1), the distributions do not vary significantly depending on the case study considered. Small differences can be observed on the estimated maximum values: for the October case the simulated maximum reflectivities are higher. On the other hand, considering the different configurations of EMVORADO, the use of Mie scattering generally produces a distribution with higher reflectivity values. By activating attenuation, values between 25^{th} and 75^{th} percentiles are realigned with other configurations, but values above 95^{th} percentiles are all limited to below 50 dBZ. For the configurations with the Rayleigh scattering, the use of different beam propagation schemes does not bring to any significant changes.

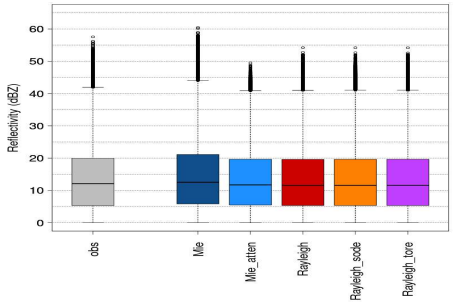

Figure 2: Boxplot calculated for October 2018 with the input analyses from KENDA cycles with the assimilation of conventional observations and radar reflectivity volumes at the analysis time.

The simulations behavior using as input analyses those derived from KENDA cycles with the assimilation of only conventional observations and radar reflectivity volumes at the analysis time (Figure 2), calculated only for October 2018, differ slightly from the previous ones. Median values are higher, but maximum values above the 95^{th} percentiles are smaller.

3 Case Study: flooding in Sardinia in October 2018

To understand in more detail how the simulated reflectivity changes according to the chosen namelist parameters, the flood that hit southern Sardinia on October 10, 2018 was analyzed. As shown in figure 3, in this part of the region, several rain gauges have measured values greater than 100 mm over the two days, with a maximum value at Santa Lucia di Capoterra of 493.4 mm. For this rain gauge the trend of the hourly accumulated precipitation (Figure 4) displays a first passage of the precipitating structures in the morning of October 9 and a persistence of the phenomena from the evening of October 10 until the end of the event.

Figure 3: Accumulated precipitation measured by rain gauges from 09/10/2018 - 00 UTC to 11/10/2019 - 00 UTC in Southern Sardinia.

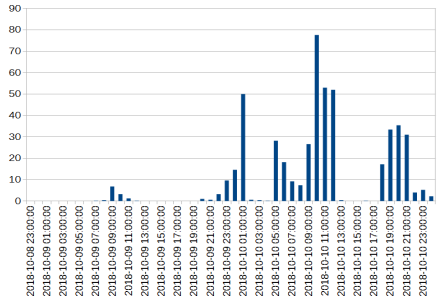

Figure 4: Accumulated hourly precipitation measured by the rain gauge located at Santa Lucia di Capoterra from 08/10/2018 - 23 UTC to 11/10/2019 - 00 UTC.

Two hours were selected and the polar volume at its lowest elevation was displayed for Armidda radar (in red, in figure 5) for the different EMVORADO configurations and depending on the input analyses.

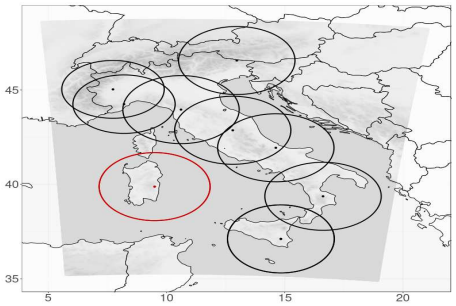

Figure 5: Armidda's radar, highlighted in red, inside the radar Italian radar network used for this study.

In figure 6 and figure 7, columns 2, 3 and 4 show the reflectivity fields simulated using Rayleigh, Mie and Mie with attenuation configurations. Simulations can be directly compared with the observation in column 1. The different rows refer to the different analyses used as input. In the first row the analyses used come from KENDA cycles with assimilation of only conventional observations (SYNOP, TEMP and AIREP). In

the second row analyses come from KENDA cycles with assimilation of conventional observations and LHN, while in the third one they comes from KENDA cycles with assimilation of conventional observations and radar reflectivity volumes at the analysis time. Figure 6 refers to 9 October at 9 UTC, while figure 7 is for 10 October at 10 UTC.

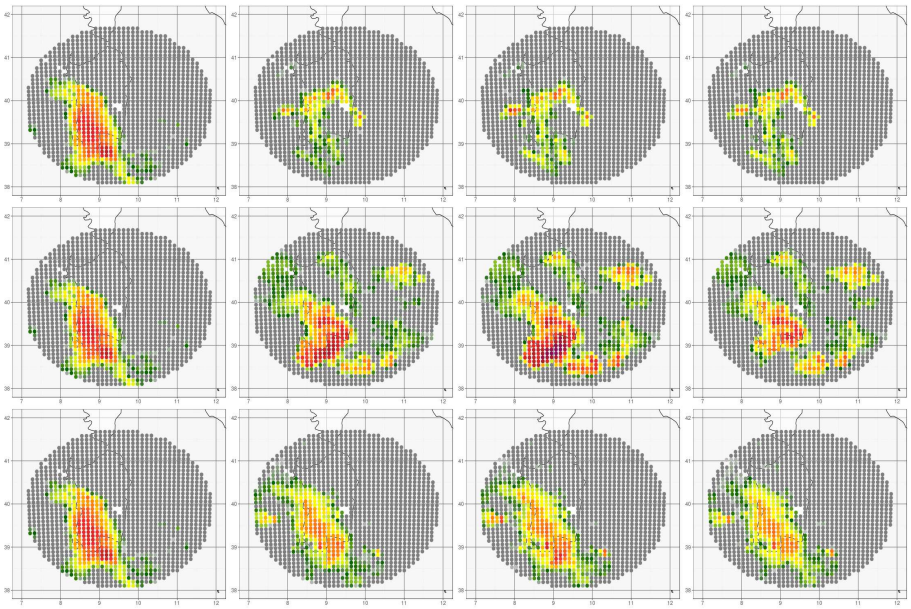

Figure 6: Observed (first column) and simulated (columns 2, 3 and 4) reflectivity of Armidda's first radar elevation by changing EMVORADO configurations (column 2: Rayleigh, column 3: Mie, column 4: Mie with attenuation) and input analyses (top row: analysis from KENDA with the assimilation of conventional observations, middle row: analysis from KENDA with the assimilation of conventional observations and LHN, bottom row: analysis from KENDA with the assimilation of conventional observations and radar reflectivity values at the analysis time) for October 9 at 9 UTC.

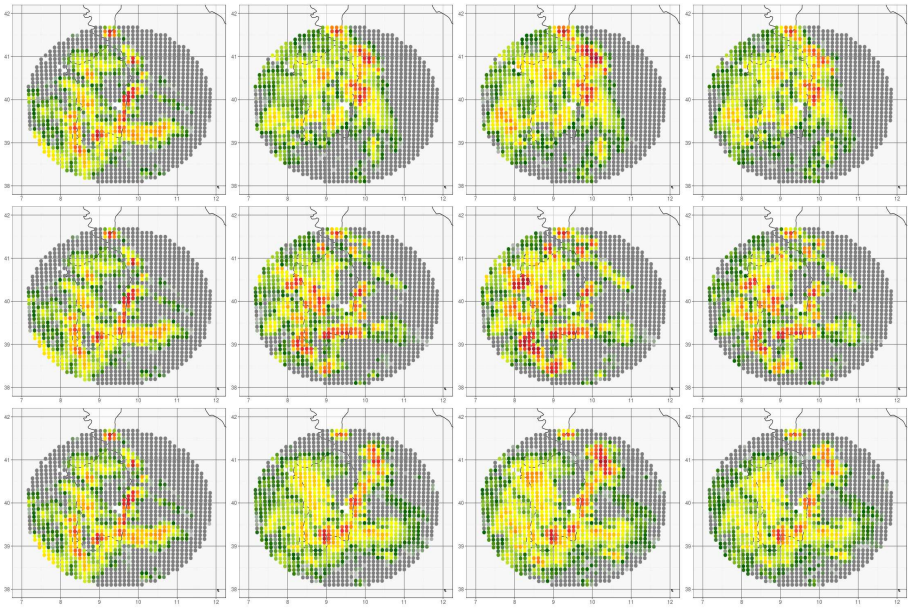

Figure 7: As fig. 6, but for October 10 at 10 UTC.

In both instants examined the structures are simulated in a more accurate way, both in terms of location and shape, if the analyses come from KENDA cycles with assimilation of radar volumes. The use of analyses with only the assimilation of conventional observations leads to the modeling of structures that have little

relevance to the observation, in particular this can be observed at the first instant.
Simulations starting from the analyses in which the LHN is used overestimate the reflectivity. This is most visible at the first instant where not only the structure in the south-west part of the domain is overestimated, but unobserved precipitation is simulated in the eastern part of the domain.
The use of Rayleigh's scattering with the analyses coming from the assimilation of radar volumes brings to a general underestimation of the field of reflectivity.
The combination of the LHN analyses and the use of the Mie configuration leads to a strong overestimation of all simulated values. As a general result, regardless of input fields, the use of attenuation improves overestimation by bringing the simulations more similar to those obtained using the Rayleigh scattering.
For this case study, comparing the obtained simulations with the observations, the use of Mie scattering provides the best results.

4 Conclusions and future work

The results obtained from this case study deviate partially from what is highlighted by the distributions of reflectivity on all events. In this case, the use of Mie scattering seems to provide the best results, while the distributions show a clear overestimation of the values with respect to the observations.
At the moment the forecasts initialized with KENDA analyses, obtained with the configuration of EMVORADO with Rayleigh scattering, provide a good improvement over the operational runs. However, the Mie scattering will be used for the case studies presented, providing a quantitative comparison between forecasts.

References

[1] Schraff, C., Reich, H., Rhodin, A., Schomburg, A., Stephan, K., Periáñez, A., and Potthast, R. 2016: Kilometre-scale ensemble data assimilation for the COSMO model (KENDA), *Q. J. Roy. Meteor. Soc.*, 142, **1453–1472**, URL `https://doi.org/10.1002/qj.2748`.

[2] Blahak, U., 2016: RADAR_MIE_LM and RADAR_MIELIB - calculation of radar reflectivity from model output. *Technical Report 28*, Consortium for Small Scale Modeling (COSMO), URL `http://www.cosmo-model.org/content/model/documentation/techReports/docs/techReport28.pdf`.

[3] Zeng, Y., 2013: Efficient radar forward operator for operational data assimilation within the COSMO-model. *Dissertation*, IMK-TRO, Department of Physics, Karlsruhe Institute of Technology, URL `http://digbib.ubka.uni-karlsruhe.de/volltexte/1000036921`.

[4] Jerger, D., 2014: Radar forward operator for verification of cloud resolving simulations within the COSMO-model. *Dissertation*, IMK-TRO, Department of Physics, Karlsruhe Institute of Technology, URL `http://digbib.ubka.uni-karlsruhe.de/volltexte/1000038411`.

[5] Zeng, Y., Blahak, U., Neuper, M. and Epperlein, D., 2014. Radar beam tracing methods based on atmospheric refractive index. *J. Atmos. Ocean. Tech.*, 31, **2650-2670**.

[6] Zeng, Y., Blahak, U. and Jerger, D., 2016. An efficient modular volume-scanning radar forward operator for NWP models: description and coupling to the COSMO model. *Quart. J. Roy. Met. Soc.*, 142, **3234-3256**, URL `http://onlinelibrary.wiley.com/doi/10.1002/qj.2904/abstract`.